Study of the Faults Stackings in the γ(f.c.c.)↔ε(h.c.p.) Martensitic Transformation

N. Bergeon, G. Guenin and C. Esnouf

INSA Lyon, Laboratoire GEMPPM, Bâtiment 502, 20 avenue A. Einstein, 69621 Villeurbanne cedex, France

Abstract. The shape memory effect exhibited by Fe-Mn-Si based alloys is due to the γ(f.c.c.)-ε(h.c.p.) martensitic transformation. The martensitic transformation induced by traction at room temperature in a Fe-16Mn-9Cr-5Si-4Ni (%mass) is here studied by optical microscopy, scanning electron microscopy, transmission electron microscopy and scanning tunnelling microscopy. The martensitic microstructure and the fine structure of the faults stackings are both studied to clarify the nucleation and growth mechanisms of martensite. The band structure of the martensite is pointed out. Inside a grain, the monopartial nature of the martensite have been demonstrated from the elementary plate to all the martensite bands. From all the observations, the pole mechanism appears to be the main mechanism of martensite nucleation.

1. INTRODUCTION

The shape memory effect is now a well-known phenomenon associated with reversible martensitic transformations. The typical shape memory alloys are Cu or Ni-Ti based, but these alloys are very expensive. Fe-based shape memory alloys have been widely investigated during the last fifteen years because of their low costs. Among them are the Fe-Mn-Si [1-4] which exhibit the γ(f.c.c.)↔ε(h.c.p.) martensitic transformation.

The well-known f.c.c.↔h.c.p. transformation is conducted by the introduction of stacking faults each second compact plane of the f.c.c. structure. Faults are created by motion of Shockley partial dislocations. All {111} compact planes laying in f.c.c. structure are able to be shear planes. Since three directions of Shockley dislocations exist in a compact plane, several different stackings can be imagined [5] :

a) The three shear directions in a {111} plane are alternated in such a way as the shear strains of individual variants cancel each other out ; that leads to a zero macroscopic shape change : self-accommodated stacking.

b) A single shear direction stacking (monopartial stacking) can also exist. It corresponds to the largest lattice shape change (homogeneous shear τ of 35.3%).

Many studies report that thermal martensite appears in self-accommodated stackings form whereas stress-induced martensite appears in monopartial stackings form [5-9]. However, the fine structure of these stackings is not clearly known. A study of this fine structure is here presented. Several microscopy techniques are used to generalise the results from the macroscopic scale to the finest one.

Many mechanisms [10-16] have been proposed to explain the multiplication and the superposition of stacking faults but none of them have been clearly demonstrated. The purpose of this article is to clarify the formation mechanism of stress-induced martensite.

2. EXPERIMENTAL METHOD

2.1 Samples preparation

The alloy used is a Fe-16%Mn-9%Cr-5%Si-4%Ni (weight%). The specimens are subjected to the following thermomechanical treatment : 850°C, 15 min + 7% cold-work + 700°C, 30 min. This kind of treatments improves the shape memory effect presented by this alloy [17-20]. For light optical microscopy, scanning tunnelling microscopy and scanning electron microscopy (SEM), austenitic samples are mechanically and electrolytically polished. The thermal martensite (ε_{th}) is produced by simple cooling ($M_s\sim0$°C) and the stress-induced martensite (ε_{st}) by tensile elongation at room temperature. The martensite fractions are measured by thermoelectric measurements [21]. For transmission electron microscopy observation, specimens are thinned after cooling or deformation. The thin foils are prepared by electrolytical thinning at 0°C in a solution of perchloric acid (10%), methanol (45%) and ethylenglycol-monobutylether (45%).

2.2 Scanning tunnelling microscopy (STM)

All the martensitic transformations create some surface topography changes. In case of the γ(f.c.c.)$\rightarrow\varepsilon$(h.c.p.) transformation, this surface topography is related to the monopartial stackings sizes. So, STM is here employed to characterise the fine structure of the stackings. STM images are performed in air using a home-built microscope, with a tunnelling current of 1 nA and a tip to sample bias of 500 mV.

The samples are polycrystalline and the grains orientations are unknown ; therefore, an angular method has been developed to analyse the data [22].

Cross sections between two points are acquired from STM images and are stored in X-Z data files (X : tip scan ; Z : tip height). The problem is that these data depend on the probable sample tilting T. Hence, an angle parameter α (figure 1) is defined in order to determine T. α is calculated for each pair of consecutive acquisition points X-Z. The maximum theoretical value of α corresponds to the maximum crystal shape change, i.e. 19.47°. Many variants can be present in one measure step and thus, α can take all the

Figure 1 : Schematic representation of X, Z, T and α parameters.

values between -19.47° and 19.47°. T appears as a constant in α values and can be easily determined. When T is known, cross sections Z'=f(X') independent from the sample tilting are drawn using the following equations 1 and 2.

$$X' = \sqrt{X^2 + Z^2} \cos\left(\arctan(Z/X) - \frac{\pi}{180}T \right) \quad (1)$$

$$Z' = \sqrt{X^2 + Z^2} \sin\left(\arctan(Z/X) - \frac{\pi}{180}T \right) \quad (2)$$

We realised some surface analysis before transformation to determine the data error. Before transformation, the surface should present no relief so, based on the results, the estimated error on Z' is $\Delta Z' = \pm 0.3$ nm.
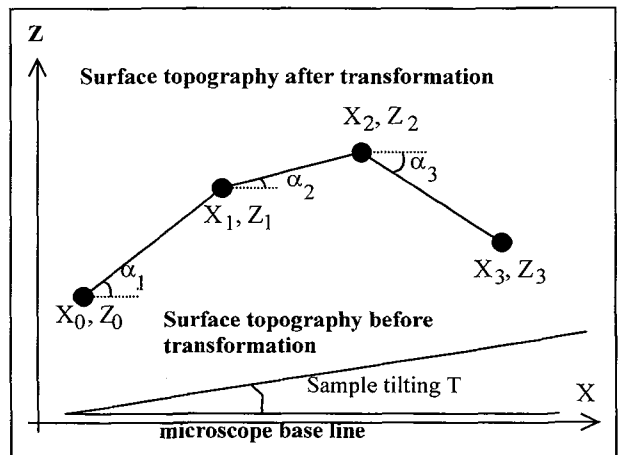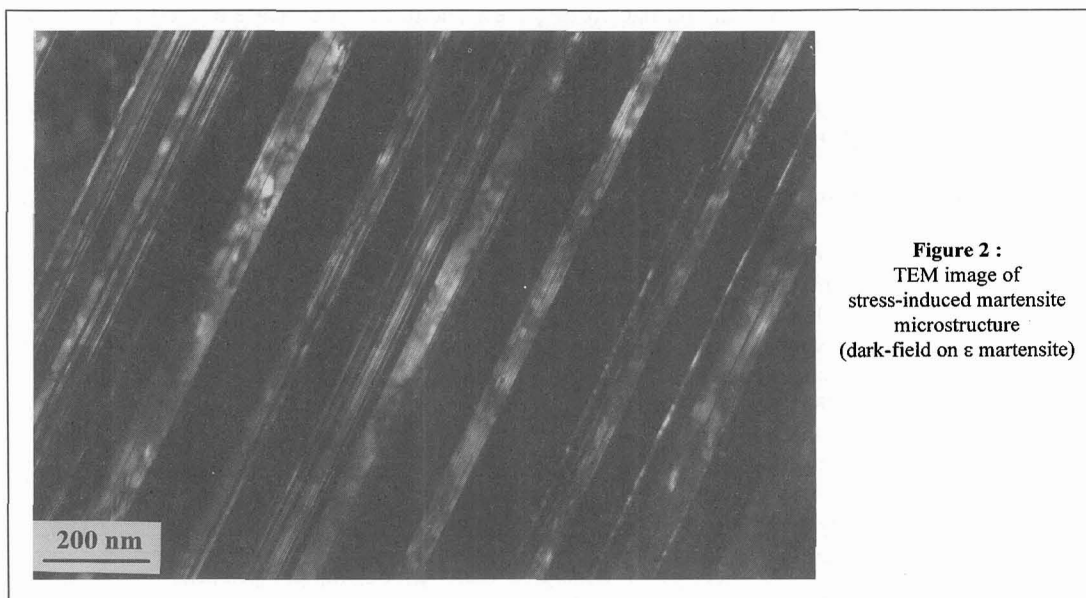
2.3 Transmission electron microscopy (TEM)

All images are realised with a zone axis along a $\langle 011 \rangle_\gamma // \langle 11\overline{2}0 \rangle_\varepsilon$ direction. In this way, half of the martensite variants are parallel to the incident beam and measurements of the martensite plates are possible. For high resolution electron microscopy (HREM), this orientation allows the ABCABC f.c.c. stackings and the ABAB h.c.p. stackings to be imaged. The corresponding plane spacings are respectively 0.207 nm (a_γ=0.359 nm) and 0.205 nm (a_ε=0.253 nm, c_ε=0.411 nm) [21]. The HREM observations have been carried out using a Jeol 2010 electron microscope with a practical resolution of 0.19 nm.

200 nm

Figure 2 :
TEM image of
stress-induced martensite
microstructure
(dark-field on ε martensite)

3. RESULTS

3.1 Microstructural study

The differences between thermal and stress-induced martensites have been previously mentioned [23]. The thermal martensite is always formed as large zones, even at low martensite fractions : increasing martensite fraction corresponds to an increase of the number of grains containing martensite. The stress-induced martensite appears as thin martensite plates randomly distributed through the material, some large zones are formed only for high martensite fractions.

The fine structure of the stress-induced martensite has been studied by TEM. A band structure is observed (figure 2) ; it corresponds to the thin martensite plates observed by light optical microscopy. The ε bands present a lamella structure consisting of a mixture of ε and γ phases : thin
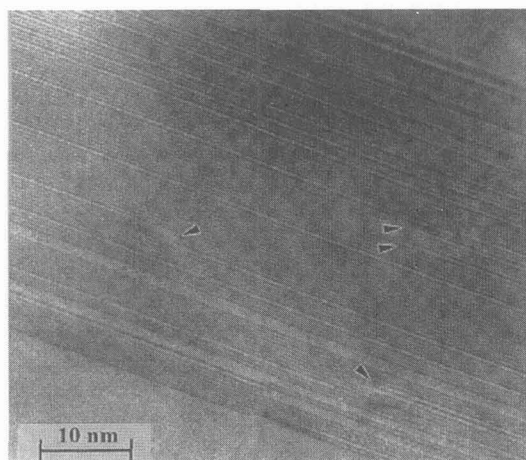

10 nm

Figure 3 : HREM image of a band of stress-induced martensite. Some defects (pointed by arrows) are observed in the martensite stacking.

martensite plates with 1.5-30 nm width are separated by very thin austenite lamellas with a width of 1-10 nm. At a deformation rate of 3% (~25% ε_{st}), the band widths vary from 35 to 350 nm ; at 7% of deformation, they vary from 300 to 500 nm. It is very important to note that the band widths increase with the deformation rate without evolution of the elementary martensite plates widths. Both TEM and HREM experiments reveal that the elementary martensite plates may contain stacking defects (figure 3).

Concerning the growth mechanism of ε stress-induced martensite, these observations are coherent with the formation sequence proposed by Kikuchi et al. [24], i.e. thin martensite plates are first formed rather uniformly through the grain and, in the further stage of transformation, some other thin plates nucleate and grow close to the first ones. This mechanism leads to a band structure containing some residual austenite between individual thin martensite plates. The thickness increase of the band does not result from a lateral growth of the martensite plates but from nucleation of some new plates close to the existing ones.

It is worth noting that most of the martensite plates go through the grain from one side to the other : that means that they stop on the grain boundaries.

3.2 Faults stacking characterisation

Concerning the surface topography, the differences between thermal and stress-induced martensites also clearly appear at the light optical microscopy and SEM scales [23]. The strain accommodation is perfect in thermal martensite on a scale of the order of 150 nm. On the same scale, there is an accumulation of little strains in stress-induced martensite.

STM is used to study the extremely fine stacking structure. The figures 4a and 4b represent some typical surface topographies measured respectively for thermal and stress-induced martensites.

The thermal martensite appears as a juxtaposition of periodic variations. The characteristic width of variations is about 50 nm, i.e. thin plates width. Crystal strains are accommodated on this width. The study of these variations reveals that the thin plates, with a width of ~50nm, correspond to a juxtaposition of very thin monopartial stackings (generally including less then 16 faults) which have different shear directions. These monopartial stackings are alternated in such a way that there is no global deformation of the surface.

Figure 4 : Surface topographies created by the martensitic transformation
a) Thermal martensite   b) Stress-induced martensite

The surface topography corresponding to stress-induced martensite is clearly higher than the thermal martensite corresponding one. A characteristic width of ~50 nm also appears and the deformation is homogeneous on this width, i.e. ~125 faults. It corresponds to an accumulation of deformations associated with large monopartial stackings. Compared with the widths measured by TEM, a size of 50 nm corresponds to one or a few number of elementary martensite plates. It is very interesting to note that the same shearing direction appears on many successive characteristic widths, extending the observation of monopartial elementary plates to monopartial ε bands.
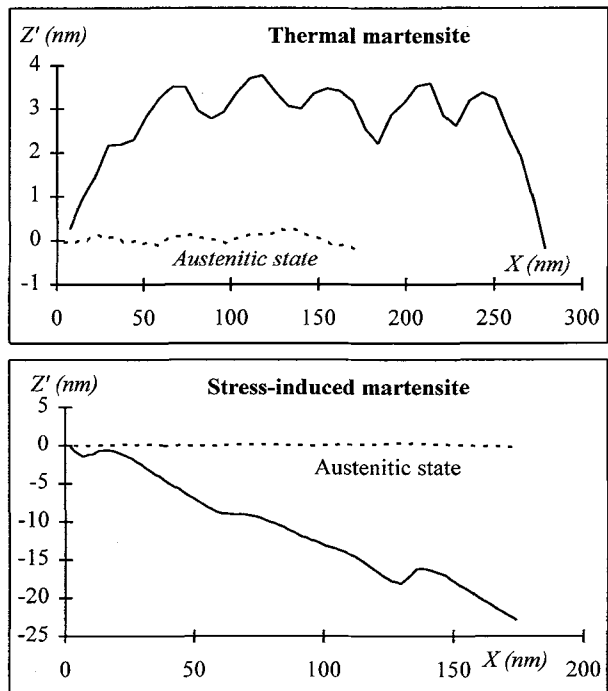
4. DISCUSSION

The analysis of the stackings have clearly shown the monopartial nature of the ε_{st} martensite. An uniform spatial distribution of martensite plates should then be more logical than this band structure because of the repulsive interaction between the elementary martensite plates. This characteristic may result from a specific nucleation mechanism. Many mechanisms of formation and superposition of stacking faults have been proposed [10-16] but, up to now, none of them have been really proved. Among these mechanisms, the pole mechanism [12-13] is the most coherent with our observations.

The pole mechanism supposes the existence of a a/2<112> dislocation (pole dislocation) fixed in a compact plane (for example resulting from the junction of 2 perfect a/2<110> dislocations moving in different {111} planes). A partial dislocation gliding in another {111} plane will be blocked on this pole ; under the stress, the 2 parts of the partial dislocation will turn around the pole. The first semi-dislocation turns clockwise and progresses down by two {111} plane distances for each complete rotation and the other turns anti-clockwise and progresses up by the same distance. Therefore, this leads to the f.c.c. to h.c.p. transformation and to perfect monopartial stackings. This mechanism is coherent with the martensite plates ends blocked on the grain boundaries because the growth center is inside the plate and not at one of its extremities.

The pole mechanism requires a pole dislocation. Even if this pole dislocation can serve for the formation of many martensite plates, these plates are grouped and located in the grain. A band structure is then created.

After the thermomechanical treatment, the austenitic state contains many stacking faults on all the {111} planes [25]. The lamella structure results from this microstructure. When an elementary plate grows, it can meet some inactivated stacking faults which can be considered as obstacles. Crossing these obstacles requires energy. The motion of a new partial dislocation under the stress is probably more favourable than the crossing of these obstacles. Therefore, the prior plate stops growing and a new plate begins. Because of the stress direction (Schmidt factor), this new plate is formed by rotation of a partial dislocation of the same Burgers vector than the first one : the group of these two plates is perfectly monopartial. The initiating stacking faults are randomly disposed on the close-packed planes (i.e. A, B or C type) so, nothing implies the coherence of the h.c.p. stackings formed by two independent partial dislocations : some thin lamellas of f.c.c. phase remain between independent plates. Depending on the local configuration of partial dislocations and stresses, some obstacles can be crossed ; this leads to the stacking defects observed in figure 4. The studies completed by Ogawa et al. [26] concerning the influence of the thermomechanical treatment on the microstructure of the martensite support this hypothesis. In case of no thermomechanical treatment, the austenitic state contains few stacking faults and residual f.c.c. lamellas are not observed. When a growing plate meets an obstacle, the stress can not be relaxed by activation of a new plate ; the obstacle is then crossed, leading to large martensite plates containing many defects. Moreover, thermomechanical [21] or training [19] treatments - which have the similar influence on the austenitic microstructure - induce a decrease of the critical stress for the martensite formation : the ability to create new plates instead of crossing obstacles can explain this decrease.

It is worth noting that the pole mechanism has been directly observed by Hoshino et al. [27] in Fe-Mn-Si single crystals previously thermomechanically treated.

5. CONCLUSION

The γ-ε martensitic transformation in a Fe-16%Mn-9%Cr-5%Si-4%Ni (%mass) has been studied using optical microscopy, scanning electron microscopy, scanning tunnelling microscopy, conventional and high resolution electron microscopy. Both the microstructure and the stackings characteristics have been analysed.

The monopartial nature of the stress-induced martensite has been demonstrated from the scale of elementary martensite plates to all the martensite plates of the grain. Considering the monopartial nature of stress-induced martensite and the microstructural observations, the pole mechanism seems to be the principal mechanism of stress-induced martensite formation.

References

[1]   Sato A., Chishima E., Soma K., Mori T., *Acta Metallurgica* 1982 **30** (1982) pp. 1177-1183.
[2]   Otsuka H., *Mater. Res. Soc. Symp. Proc.* **246** (1992) pp. 309-319.
[3]   Guénin G., *Journal de Physique IV* **5** (1995) 325.
[4]   Sato A., Mori T., *Materials Science and Engineering* **A146** (1991) pp. 197-204.
[5]   Yang J.H., Wayman C.M., *Materials Characterization* **28** (1992) pp. 23-35.
[6]   Yang J.H., Wayman C.M., *Materials Characterization* **28** (1992) pp. 37-47.
[7]   Putaux J.L., Chevalier J.P., *Acta Mater.* **44** (1996) pp. 1701-1716.
[8]   Maki T., Tsuzaki K., in Proceedings of the International Conference on Martensitic Transformations, Monterey, 1992, edited by the Monterey Institute for Advanced Studies (1993), pp. 1151-1162.
[9]   Sato A., Chishima E., Yamaji Y., Mori T., *Acta Metallurgica.* **32** (1984) pp. 539-547.
[10] Fujita H., Ueda S., *Acta Metallurgica* **20** (1972) pp. 759-767.
[11] Delamotte E., Altstetter C., *Transactions of the metallurgical society of AIME*, **245** (1969) pp. 651-659.
[12] Seeger A., *Z. Metallkunde* **44** (1953) pp. 247-255.
[13] Seeger A., *Z. Metallkunde* **47** (1956) pp. 653-660.
[14] Bollman W., *Acta Metallurgica* **9** (1961) pp. 972-975.
[15] Mahajan S., Green M.L., Brasen D., *Metallurgical Transactions A* **8A** (1977) pp. 283-293.
[16] Lysak L.I., *Fiz.Metal. Metall.* **20** (1967) pp. 547-554.
[17] Yang J.H., Chen H., Wayman C.M., *Metallurgical Transactions A* **23** (1992) pp. 1431-1437.
[18] Moriya T., Kimura H., Ishizaki S., Hashizume S., Suzuki S., Suzuki H., Sampei T., *Journal de Physique IV* **C4-1** (1991) pp. 433-437.
[19] Otsuka H., Murakami M., Matsuda S., in Materials Research Society International Meeting on Advanced Materials, 1989,. edited by M. Doyama, S. Somiya and R.P.H. Chang (Pittsburgh : Materials Research Society, 1989) pp. 451-455.
[20] Inagaki H., *Z. Metallkd* **83** (1992).pp. 90-96.
[21] Federzoni L., Thesis : Institut National des Sciences Appliquées de Lyon, 1993, 265p.
[22] Bergeon N., Robach Y., Esnouf C., Guénin G. Porte L., *To be published in Journal of Materials Science Letters*.
[23] Bergeon N., Guénin G., *Journal de Physique III* **C8-5** (1995) pp. 439-444.
[24] Kikuchi T., Kajiwara S., Tomota Y., *Materials Transactions* **36** (1995) pp. 719-728.
[25] Bergeon N., G. Guénin, C. Esnouf, *Submitted to Materials Science and Engineering*
[26] Ogawa K., Kajiwara S., *Materials Transactions* **34** (1993) pp. 1169-1176.
[27] Hoshino Y., Nakamura S., Ishikawa N., Sato A., *Materials Science Forum* **56** (1990) 643.